

# THE EFFECT OF MICROSTRUCTURE AND PORE MORPHOLOGY ON MECHANICAL AND DYNAMIC PROPERTIES OF FERROUS P/M MATERIALS

Tina M. Cimino, Amie H. Graham and Thomas F. Murphy

Presented at pM2TEC '98  
International Conference on Powder Metallurgy & Particulate Materials May 31 - June 4,  
1998 Las Vegas, NV USA

## ABSTRACT

Fatigue testing was performed on FN-0205 premixes in order to evaluate the effect of pore structure and processing method on the fatigue properties. The premixes were made with two-nickel sources:

- mean particle size of 4  $\mu\text{m}$
- mean particle size of 50  $\mu\text{m}$

Metallographic analysis was performed to quantify the pore structure. The following parameters were examined: pore size, pore shape, mean pore spacing and average pore size.

Previous work, which examined a variety of materials, indicated that predicting the fatigue strength of a material is a complex relationship between the type and strength of the microstructural constituents, as well as stereological parameters such as mean pore spacing and pore size.

This paper attempts to determine to what extent each of the above parameters influences the fatigue strength of P/M materials.

## INTRODUCTION

Due to the increasing trend toward higher densities and high performance applications, understanding how the fatigue properties of P/M materials are affected by alloying additions and processing techniques is becoming increasingly important.

Previous studies have indicated that fatigue properties appear to be influenced by density and sintering temperature as well as stereological parameters.

In the present study, which is part of an ongoing program to evaluate dynamic properties of P/M materials at Hoeganaes, the fatigue properties of FN-0205 and FC-0208 conventional premixes with various copper and nickel particle sizes were evaluated. The use of different copper and nickel particle sizes provided the ability to modify the porosity size and spacing. The fatigue properties were assessed in relationship to ultimate tensile strength and key stereological parameters.

## MATERIALS AND PROCESSING

The compositions of the conventional premixes analyzed in this study are detailed in Table I. In order to generate the various copper sizes that were used, a sample of ACuMet minus 200 mesh atomized copper was screened into three distinct particle size ranges, with the mean

particle sizes listed in Table I. The nickel used for mixes D and E was Novamet / Type 4SP and Inco 123 respectively. The graphite utilized in the study was Asbury 3203 SCR HS and each mix included 0.75 w/o Lonza Acrawax.

Fatigue and tensile samples for materials A through E were compacted at various pressures to attain comparable density levels. Specimens were sintered in a 75 v/o H<sub>2</sub>/ 25 V/O N<sub>2</sub> atmosphere for thirty minutes at temperatures of 2050°F (1120°C) and 2300°F (1260°C).

The dogbone specimens for tensile testing were utilized as compacted while the fatigue specimens were machined and ground to size, from a 0.45 inch x 0.45 inch x 3.5 inch nominal sized specimen, following the sintering operation.

After compaction and sintering, density was determined on samples by the immersion method outlined in MPIF Standard 42<sup>3</sup>. The dimensions of the fatigue specimen are shown in Figure 1. The as-sintered tensile properties were determined according to MPIF Standard 10 utilizing a 60,000-pound Tinius Olsen universal tensile tester<sup>3</sup>

Fatigue testing was performed on six randomly selected Fatigue Dynamics RBF-200 machines at a rotational speed of 8,000 rpm. A "runout" for the test was considered to be 107 cycles. The staircase method of testing was regulated so that there were both failures and "runouts" at a minimum of two stress levels. The percentage of failures for each stress level was calculated and plotted on a log-normal graph. From these plots, the fatigue endurance limit (FEL) at 50% and 99.9% was determined. (Extrapolation was used to estimate 99.9% FEL). The 50% FEL represents the stress level where 50% of the specimens will break and 50% will "runout". The 99.9% FEL represents the stress level where 99.9% of the specimens will "runout" and 0.1% will break.

## RESULTS

The tensile and fatigue properties for all test materials are summarized in Tables II and III, as well as the 50% FEL as a percentage of the ultimate tensile strength at sintering temperatures of 2050°F (1120°C) and 2300°F (1260°C). Due to the variability between the specimen types, the density of the tensile specimens did not exactly match that of the fatigue specimens. To correlate the data, tensile properties were interpolated from available data.

Specimens of all test materials underwent metallographic analysis. Pore structures of the unetched microstructures were analyzed with a Leitz TAS+ automated image analysis system according to established techniques by DeHoff and Aigeltinger.<sup>4</sup> Mean pore spacing and pore size were determined from stereological analysis and the results for Mixes D and E are summarized in Table IV. Pore shape was determined by the form factor:

$$\text{Form Factor} = 4 \pi A / P^2$$

Where

A = Area of pore

P = Circumference of pore in plane of analysis

A shape factor of 1 represents a circular pore in the plane of analysis and as the number decreases from 1, the degree of irregularity increases. The form factor can predict the degree of

irregularity, but not symmetry.

In addition to quantitative analysis of the unetched microstructure, optical microscopy was conducted on selected samples in the etched condition.

## DISCUSSION

### Sintered Density and Sintering Temperature

Sintered density versus 50% FEL for Mixes D and E is plotted in Figure 2. The 50% FEL was selected because it provides an appropriate comparison of data between materials while limiting the potential extrapolation error that might be associated with 99.9% data.

For both Mixes D and E, the fatigue strength was increased with increasing density. At a sintering temperature of 2050°F (1120°C), Mixes D and E show approximate increases of 2150 psi and 2400 psi (14.8 MPa and 16.5 MPa), respectively for each 0.1 g/cm<sup>3</sup> increase in density. At 2300°F (1260°C) Mixes D and E show approximate improvements in 50% FEL of 2400 psi and 2800 psi (16.5 MPa and 19.3 MPa), respectively for each 0.1-g/cm<sup>3</sup> increase in sintered density. This indicates that the influence of density on 50% FEL is slightly stronger for Mix E and is more pronounced at the higher sintering temperature. Previous work that was done with Mixes A, B and C indicated that, for the copper containing materials, the influence of density on 50% FEL is also stronger as the sintering temperature is increased. However, in contrast to Mixes D and E, for the copper containing materials the influence of density on 50% FEL was stronger as the copper particle size increased?

For Mix D (mean particle size 50 μm), the fatigue performance, at a constant density level, was comparable or increased slightly as the sintering temperature increased from 2050°F (1120°C) to 2300°F (1260°). For Mix E, (mean particle size 4 μm), the 50% FEL was higher than Mix D at all density levels; however the values decreased with increasing sintering temperature, except at the highest density level. These results confirmed previous fatigue studies with materials containing standard grade nickel, but also highlight the benefit of nickel rich areas in arresting fatigue crack propagation. 1,2

### Ultimate Tensile Strength

The relationship between ultimate tensile strength and 50% FEL for Mixes D and E is shown in Figure 3. For Mix D, the ultimate tensile strength increased an average of 32% and the 50% FEL increased approximately 6%, at a given density level, as the sintering temperature increased from 2050°F (1120°C) to 2300°F (1260°C). For Mix E, the ultimate tensile strength increased only an average of 8% and the 50% FEL remained fairly constant, at a given density level, as the sintering temperature increased from 2050°F (1120°F) to 2300°F (1260°C). This seems to suggest that nickel rich areas and microstructural homogenization are critical features for dynamic properties.

Figure 4 highlights 50% FEL as a percentage of UTS for Mixes A through E. This property clearly varies with premix composition and sintering temperature. For the copper containing materials, Mixes A, B and C, 50% FEL as a percentage of UTS increases as the copper particle size decreases as well as with increasing sintering temperature. Mixes D and E, tend to show the opposite trend. The 50% FEL as a percentage of UTS increases as the nickel particle size increases and the sintering temperature decreases. This discrepancy is most likely due to the difference between the alloy rich areas. Due to the fact that copper melts during sintering,

copper rich areas easily diffuse into the iron matrix and tend to leave behind large pores in the microstructure. These pores become more predominant as the copper particle size increases. Nickel does not melt during sintering and homogenization must occur by a much slower diffusion mechanism. The experimental data support the theory that pore morphology and microstructure influence fatigue properties.

### **Stereological Parameters**

Stereological parameters, including pore shape, mean pore size and mean pore spacing were examined to evaluate the effects of pore structure on fatigue properties.

Plots of pore shape at 2050°F (1120°C) and 2300°F (1260°F) for Mixes D and E compacted to a green density of 7.2 g/cm<sup>3</sup> are shown in Figure 5. As expected, with increasing sintering temperature the pore shape becomes more circular. It also appears that the nickel particle size has very little effect on the pore size which seems to correlate with previous work which analyzed Mixes A, B and C.

A previous study, which analyzed Mixes A, B and C found no relationship between the number of pores per unit area and the fatigue endurance limit? For the present study, the analysis focused on the average pore size, rather than the number of pores per unit area. This relationship is plotted in Figure 6. Clearly, as the average pore size decreases the 50% FEL increases. The data also indicate that for a given 50% FEL, Mix D that contains the larger nickel, has a larger mean pore size. The 50% FEL for Mix D also appears to be less affected by sintering temperature.

The cumulative % pore size for materials compacted to a green density of 7.2 g/cm<sup>3</sup> and sintered at temperatures of 2050°F (1120°C) and 2300°F (1260°C) is plotted in Figure 7. In general, the cumulative % pores size increases as the sintering temperature is increased. However, Mix E, which contains the standard grade nickel, appears to have a larger overall pore structure.

The mean pore spacing versus the 50% FEL is plotted in Figure 8. For Mixes D and E at sintering temperatures of 2050°F (1120°C) and 2300°F (1260°C), as the mean pore spacing increased, the 50% FEL increased. However, for a given material, as the sintering temperature was increased, the mean pore spacing increased with little or no corresponding increase in 50% FEL. This correlates with previous work that was done on a wide range of premixes and seems to indicate that although there is a relationship between mean pore spacing and fatigue properties; this is not the only factor in determining fatigue properties.

## Microstructure

Photomicrographs of Mixes D and E at a density of  $6.8 \text{ g/cm}^3$  and sintering temperatures of  $2050^\circ\text{F}$  ( $1120^\circ\text{C}$ ) and  $2300^\circ\text{F}$  ( $1260^\circ\text{C}$ ), are shown in Figure 9. At  $2050^\circ\text{F}$  ( $1120^\circ\text{C}$ ), both mixes contain nickel rich areas, with Mix D appearing to have a larger pore structure. As the sintering temperature was increased to  $2300^\circ\text{F}$  ( $1260^\circ\text{C}$ ), the microstructure of Mix E appears to have homogenized while large nickel rich areas are still clearly visible in Mix D.

A photomicrograph of the fatigue crack propagation for Mix E at a density of  $6.8 \text{ g/cm}^3$  and sintered at  $2050^\circ\text{F}$  ( $1120^\circ\text{C}$ ) is shown in Figure 10. The propagation of the crack does seem to favor a path around the nickel rich areas. This supports the theory that the nickel rich areas enhance fatigue performance.

This continuing study of fatigue properties in P/M materials provides more evidence for the fact that the fatigue endurance limit of a material is a complex relationship between many factors.

Future work will include point counts of all samples for Mixes D and E to determine if there is any relationship between the amount of ferrite, pearlite and martensite contained in the materials and the fatigue properties. Grain size analysis will also be conducted.

## CONCLUSIONS

1. As with previous work done on FC-0208 premixes, as the density of the FN-02O5 premixes increased, the fatigue properties increased. However, as the sintering temperature was increased from  $2050^\circ\text{F}$  ( $1120^\circ\text{C}$ ) to  $2300^\circ\text{F}$  ( $1260^\circ\text{C}$ ), for Mixes A, B, C, (the copper containing materials) and Mix D (mean particle size  $50 \mu\text{m}$ ), the fatigue properties also increased. The opposite trend was seen with Mix E, which contained the Inco 123 nickel (mean particle size  $4 \mu\text{m}$ ).
2. Mix D showed a 32% average increase in UTS with a corresponding 6% increase in 50% FEL as the sintering temperature increased from  $2050^\circ\text{F}$  ( $1120^\circ\text{C}$ ) to  $2300^\circ\text{F}$  ( $1260^\circ\text{C}$ ). Mix E showed only an 8% average increase in UTS with no corresponding increase in 50% FEL as the sintering temperature increased from  $2050^\circ\text{F}$  ( $1120^\circ\text{C}$ ) to  $2300^\circ\text{F}$  ( $1260^\circ\text{C}$ ).
3. FEL as a percentage of the ultimate tensile strength varied significantly for Mixes A through E. The data indicates that this is most likely due to differences in pore morphology and the different diffusion mechanism of copper and nickel during the sintering process.
4. All work done to date indicates that differences in nickel and copper particle size have no significant effect upon pore shape. There do appear to be relationships between average pore size, mean pore spacing and 50% FEL.
5. This study strongly suggests a relationship between microstructural homogeneity and fatigue properties. Future work will examine the effect of microstructural constituents such as ferrite, pearlite and martensite in more detail.

## ACKNOWLEDGMENTS

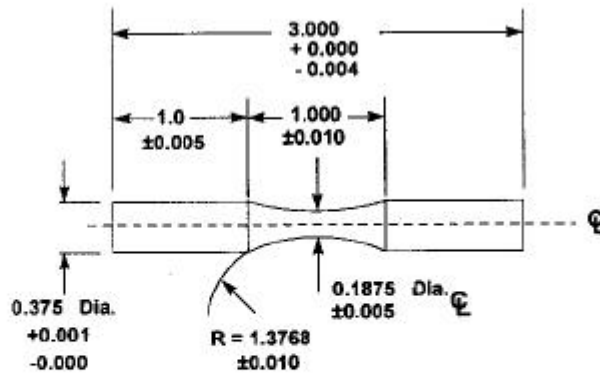
The authors of this manuscript wish to recognize the contributions of Steve Kolwicz and Jerry Golin to this paper. Their timely preparation of the metallographic samples is much appreciated.

## REFERENCES

1. Rutz, H.G., Murphy, T.F., Cimino, T.M., "The Effect of Microstructure on Fatigue Properties of High Density Ferrous Materials", *Advances in Powder Metallurgy and Particulate Materials-1996*, Vol. 4, pp 13-375 13-389, Metal Powder Industries Federation, Princeton, NJ.
2. Cimino, T.M., Rutz, H.G., Murphy, T.F.1 Graham, A.H., "The Effect of Microstructure on Fatigue Properties of Ferrous P/M Materials", *Advances in Powder Metallurgy and Particulate Materials-1997*, Vol. 2, pp 13-137 13-149, Metal Powder Industries Federation, Princeton, NJ.
3. "Standard Test Methods for Metal Powders and Powder Metallurgy Products", Metal Industries Federation, Princeton, NJ, 1996.
4. DeHoff, R.T., Aigeltinger, E.H., "Experimental Quantitative Microscopy with Special Applications to Sintering", *Perspectives in Powder Metallurgy--Volume 5--Advanced Experimental Techniques in Powder Metallurgy*, pp81-137, Plenum Press, New York--London, 1970.

**Table I: Premix Compositions**

Material	Base Powder	Nominal Premix Additions				
		Graphite (w/o)	Copper (w/o)	Copper Particle Size (µm)	Nickel (w/o)	Nickel Particle Size (µm)
A	Ancorsteel 1000	0.6	2.0	$d_{50} \sim 98$		----
B	Ancorsteel 1000	0.6	2.0	$d_{50} \sim 73$		----
C	Ancorsteel 1000	0.6	2.0	$d_{50} \sim 30$		----
D	Ancorsteel 85 HP	0.5	----		2.0	$d_{50} \sim 50$
E	Ancorsteel 85 HP	0.5	----		2.0	$d_{50} \sim 4$



ALL DIAMETERS TO BE CONCENTRIC WITHIN 0.001  
 SURFACE FINISH = 8 RMS (Polished Longitudinal)

Note: All Dimensions are in inches

**Figure 1: Dimensions of Rotating Bending Fatigue Specimen**

**Table II: Fatigue and Tensile Properties for FC-0205 Premixes Sintered at 2050°F (1120°C) / 2300°F (1260°C)**

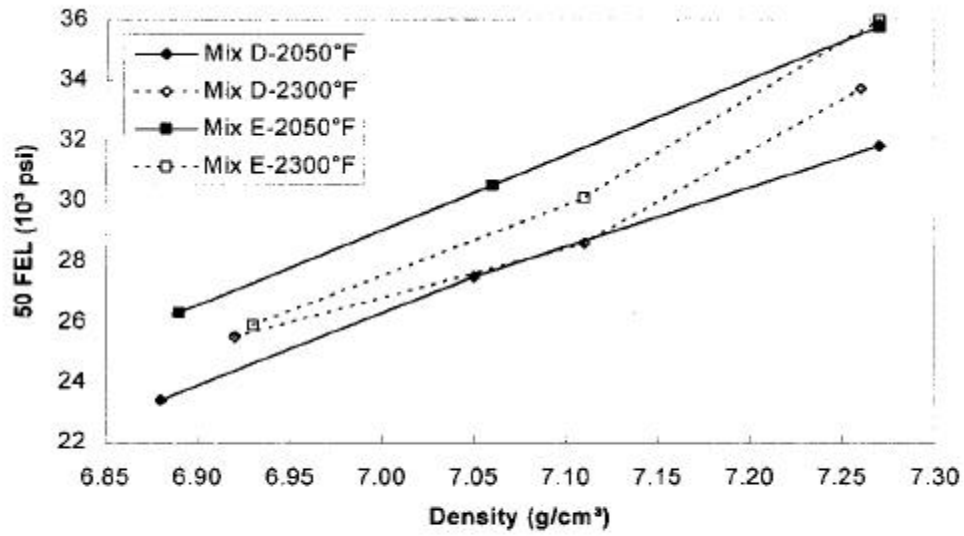
Material	Sintering Temperature (°F / °C)	Density (g/cm <sup>3</sup> )	UTS (10 <sup>3</sup> psi / MPa)	50% FEL (10 <sup>3</sup> psi / MPa)	99.9% FEL (10 <sup>3</sup> psi / MPa)	50% FEL as % UTS
A	2050 / 1120	6.89	70.0/483	25.3/174	20.3/140	36.2
		7.06	79.3/547	30.0/207	23.6/163	37.9
B		6.87	69.2/477	25.0/172	20.8/143	36.1
		7.07	78.6/542	31.6/218	25.8/178	40.1
C		6.89	72.3/498	30.6/211	24.5/169	42.3
		7.08	80.0/552	31.7/219	26.9/185	39.6
A	2300 / 1260	6.97	72.4/499	25.7/177	20.4/141	35.5
		7.14	80.0/552	34.1/235	28.4/196	42.6
B		6.94	73.0/503	29.6/204	23.4/161	40.5
		7.15	81.5/562	34.7/239	27.8/192	42.5
C		6.95	73.7/508	32.1/221	27.8/192	43.5
		7.16	87.0/600	36.1/249	29.4/203	41.4

**Table III: Fatigue and Tensile Properties for FN-0205 Premixes Sintered at 2050°F (1120°C) / 2300°F (1260°C)**

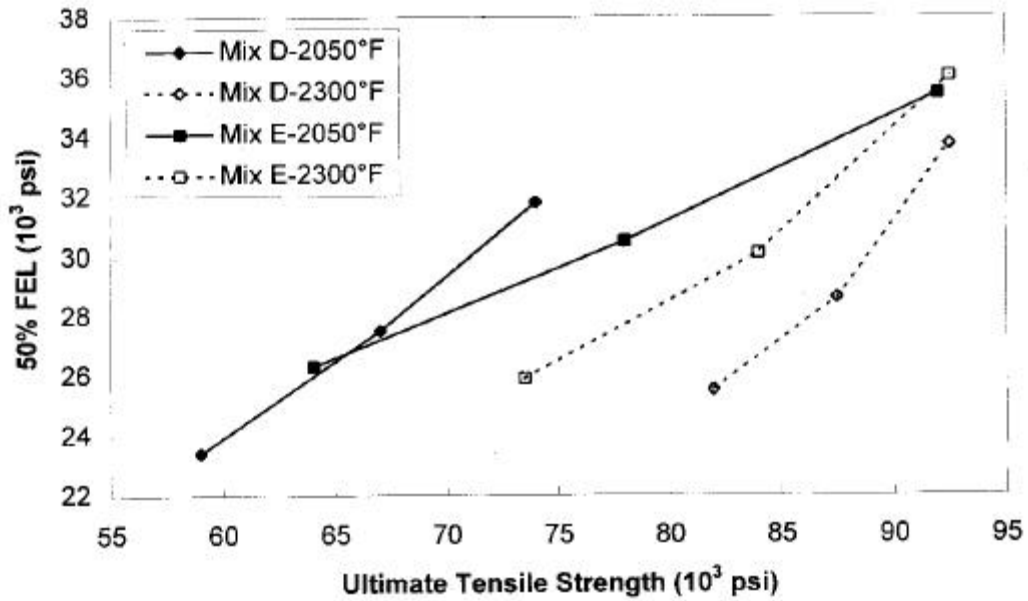
Material	Sintering Temperature (°F / °C)	Density (g/cm <sup>3</sup> )	UTS (10 <sup>3</sup> psi / MPa)	50% FEL (10 <sup>3</sup> psi / MPa)	99.9% FEL (10 <sup>3</sup> psi / MPa)	50% FEL as % UTS
D	2050 / 1120	6.88	59.0/407	23.4/161	21.2/146	38.9
		7.05	67.0/462	27.5/189	20.2/139	38.2
		7.27	74.0/510	31.8/219	24.9/172	43.0
E		6.89	64.0/441	26.3/181	23.7/163	34.5
		7.06	78.0/537	30.5/210	23.4/161	35.0
		7.27	92.0/634	35.4/244	31.4/216	37.5
D	2300 / 1260	6.92	82.0/565	25.5/176	19.4/134	31.1
		7.11	87.5/603	28.6/197	22.5/155	31.3
		7.26	92.5/637	33.7/232	28.7/198	34.3
E		6.93	73.5/506	25.9/178	19.6/135	32.6
		7.11	84.0/579	30.1/207	27.5/189	32.6
		7.27	92.5/637	36.0/248	31.9/220	36.0

**Table IV: Stereological Data**

Material	Sintering Temperature (°F) / (°C)	Density (g/cm <sup>3</sup> )	Mean Pore Size (µm)	Mean Pore Spacing (µm)	
D	2050 / 1120	6.88	102.2	42.4	
		7.27	44.9	48.3	
E		6.89	86.6	37.6	
		7.27	40.1	47.5	
D		2300 / 1260	6.92	78.6	48.4
			7.26	44.5	56.3
E	6.93		97.3	45.0	
	7.27		52.5	50.2	



**Figure 2: Sintered Density versus 50% FEL - Sintering Temperatures 2050°F (1120°C) / 2300°F (1260°C)**



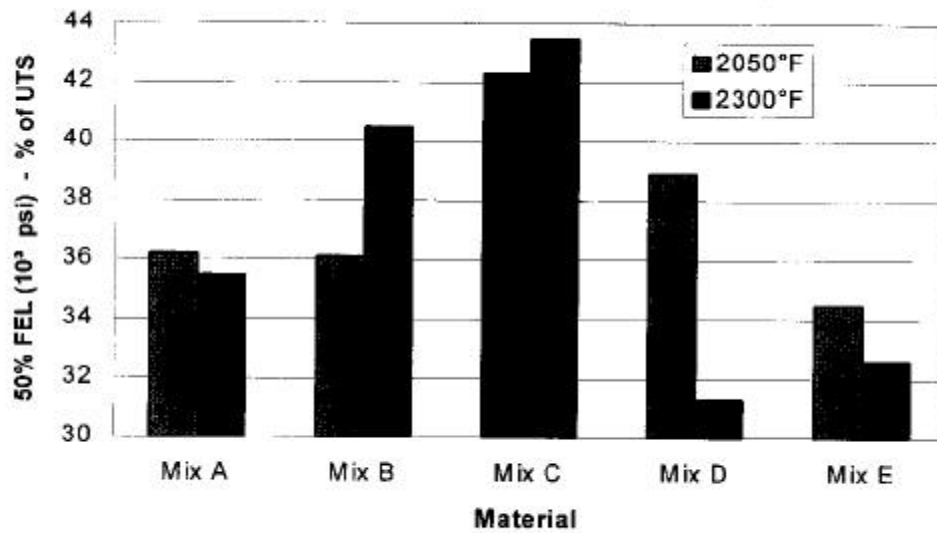


Figure 4 - 50% FEL as a Percentage of the Ultimate Tensile Strength

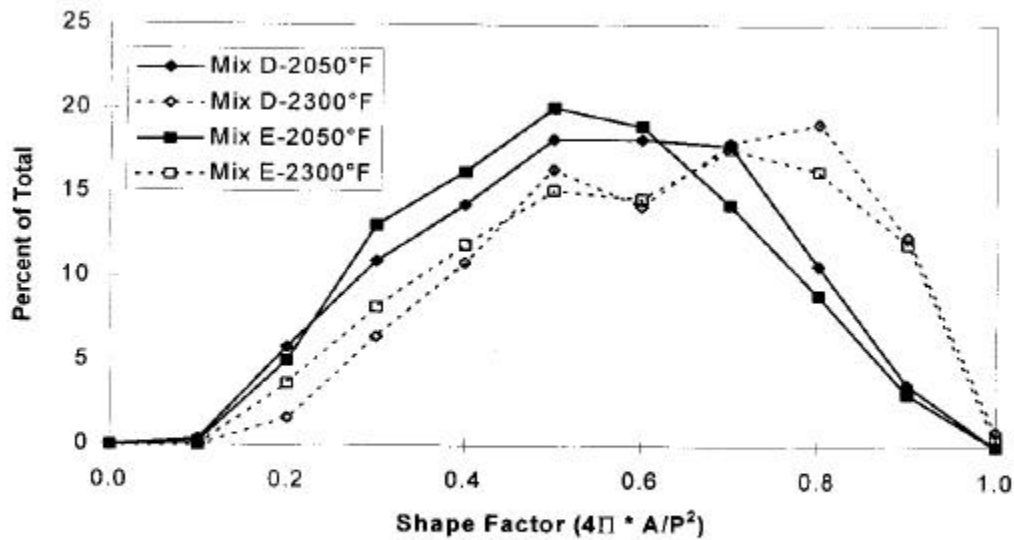


Figure 5: Pore Shape of FN-0205 Premixes - Compacted to Green Density of 7.2 g/cm<sup>3</sup>

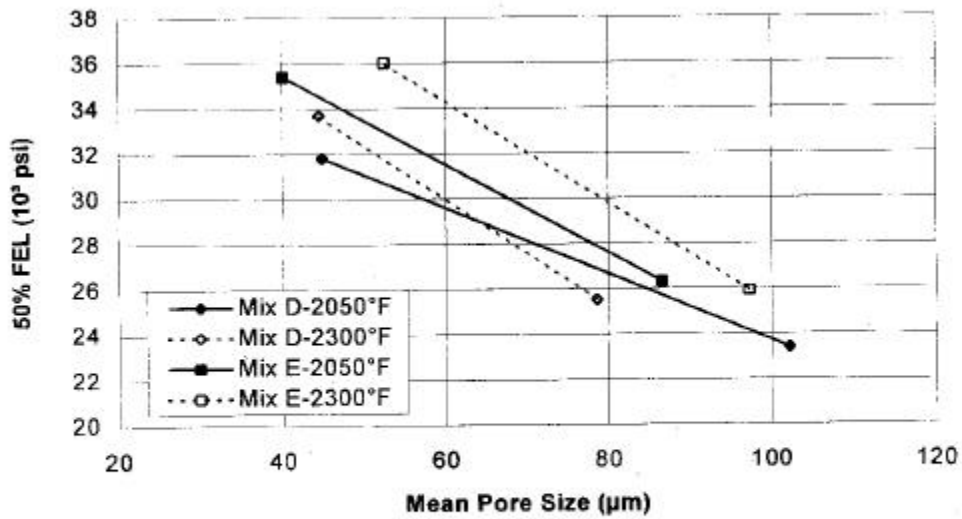


Figure 6: Mean Pore Size versus 50% FEL - FN-0205 Premixes

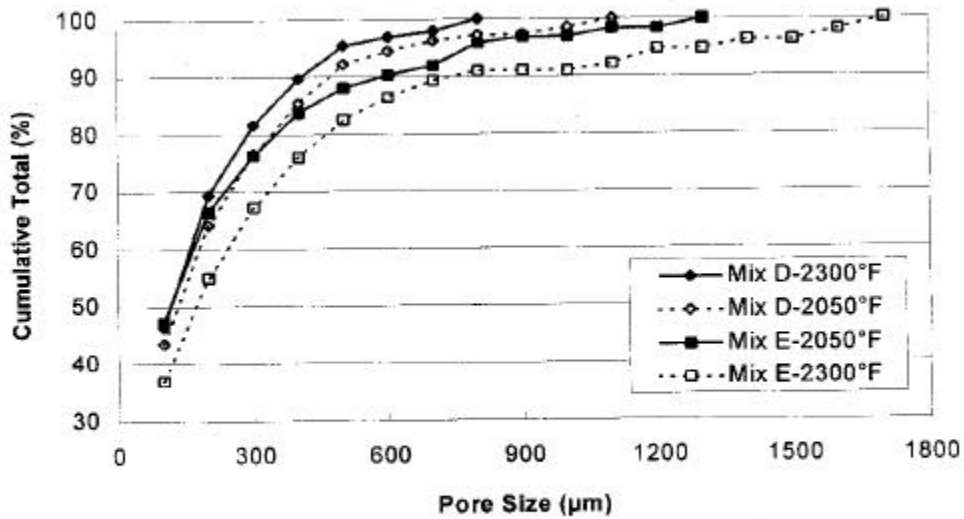
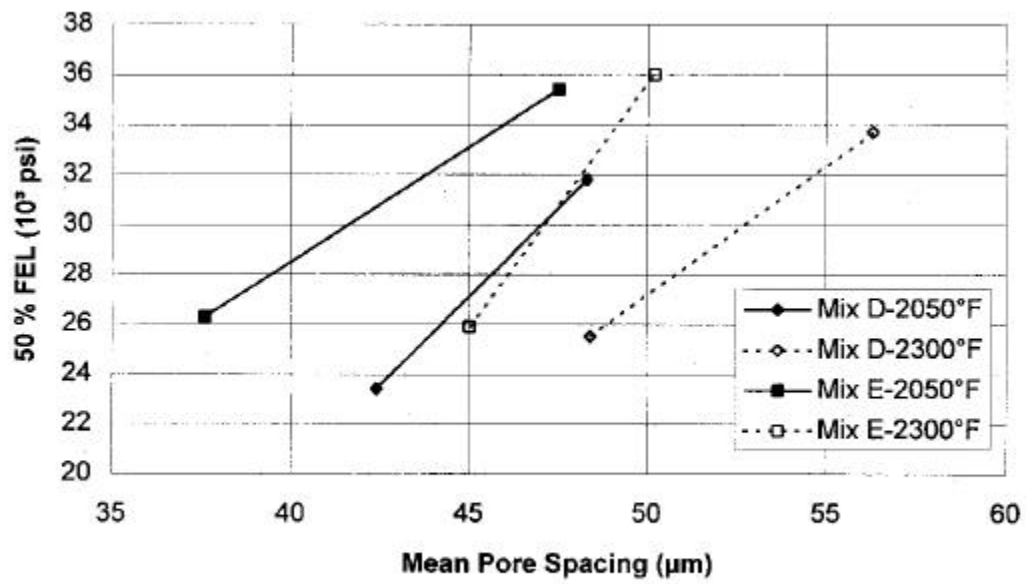
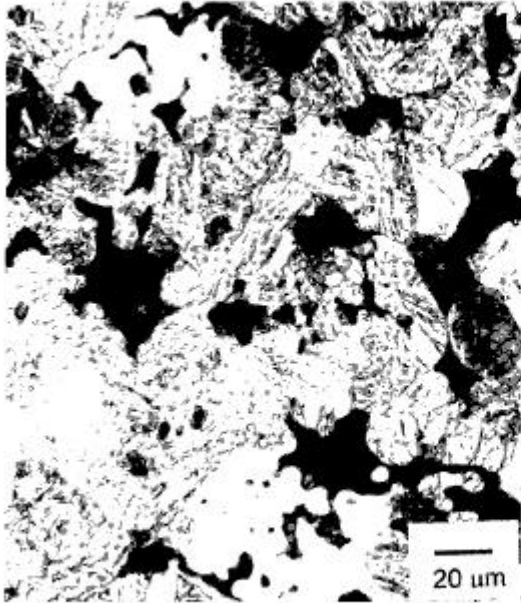


Figure 7: Pore Size versus Cumulative Total % - Sintering Temperatures 2050°F (1120°C) / 2300°F (1260°C) - Green Density 7.2 g/cm³ FN-0205 Premixes



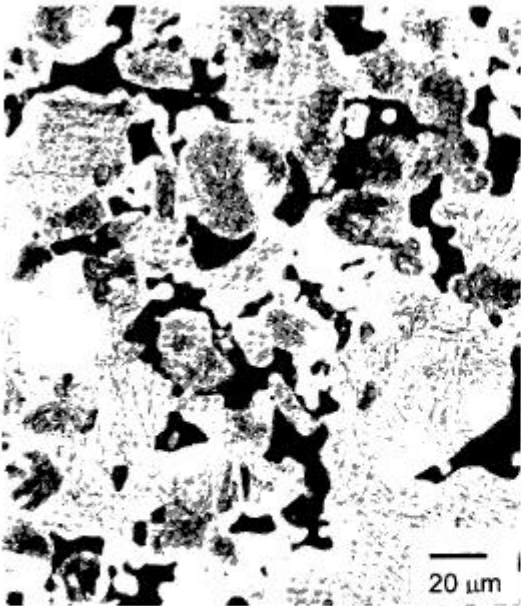
**Figure 8: Mean Pore Spacing versus 50% FEL for FN-0205 Premixes**



Mix D - 2050°F (1120°C)



Mix D - 2300°F (1260°C)



Mix E - 2050°F (1120°C)



Mix E - 2300°F (1260°C)

Figure 9: Photomicrographs of Etched Microstructures - FN0205 Premixes  
Green Density - 6.8 g/cm<sup>3</sup> - Sintering Temperatures 2050°F (1120°C) /  
2300°F (1260°C)

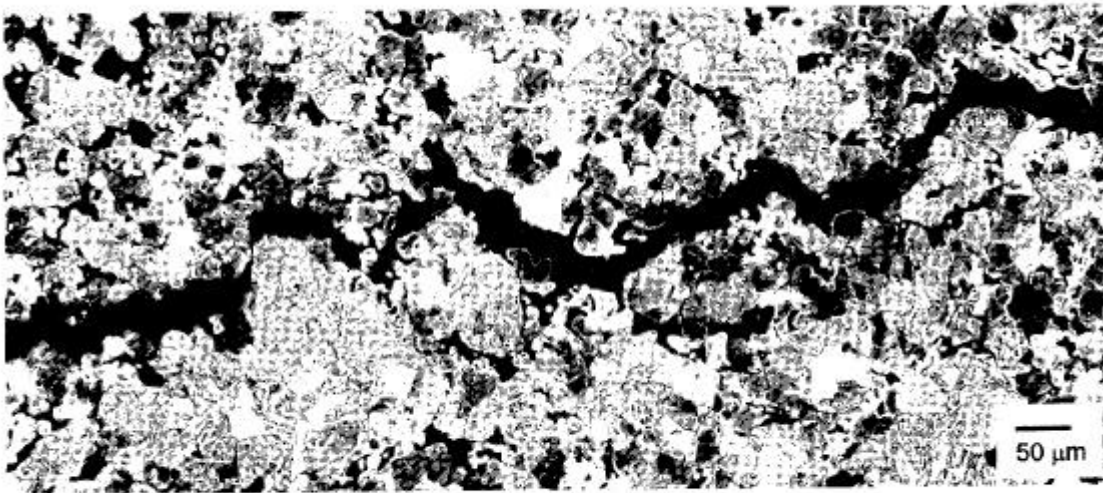


Figure 10: Photomicrograph of crack propagation - Mix E  
Green Density -  $6.8 \text{ g/cm}^3$  / Sintering Temperature  $2050^\circ\text{F}$  ( $1120^\circ\text{C}$ )